MDPI

NIR to LWIR Dichroic Beamsplitter Designed and Manufactured for Space Optical Remote Sensor

Lin Jiang [1], Yang Qin [1], Tianyan Yu [1,*], Weibo Duan [1,2,*] and Dingquan Liu [1]

1 Shanghai Key Laboratory of Optical Coatings and Spectral Modulation, Shanghai Institute of Technical Physics, Chinese Academy of Sciences, Shanghai 200083, China; jianglin@mail.sitp.ac.cn (L.J.); unpass@126.com (Y.Q.); dqliu@mail.sitp.ac.cn (D.L.)
2 College of Mechanical Engineering, Chongqing University of Technology, Chongqing 400054, China
* Correspondence: tyan_yu@mail.sitp.ac.cn (T.Y.); duanweibo@mail.sitp.ac.cn (W.D.)

Abstract: The infrared dichroic beamsplitter plays an important role in infrared multi-band imaging systems, especially for infrared remote sensing. This paper presents the design and preparation of a dichroic beamsplitter that is capable of reflecting near infrared (NIR) and shortwave infrared (SWIR), and transmitting medium wave infrared (MWIR) as well as longwave infrared (LWIR). A single crystal germanium (Ge) sheet is used as the substrate of the dichroic beamsplitter, while Ge, zinc sulfide (ZnS) and ytterbium trifluoride (YbF$_3$) are selected as coating materials. The average reflectance of the dichroic beamsplitter is more than 95% in bands 1.28 to 1.38 μm, 1.58 to 1.83 μm, and 1.95 to 2.32 μm, and the average transmittance is more than 92% in bands 3.7 to 6.2 μm and 7.5 to 12.5 μm at an incident angle of 45°. The dichroic beamsplitter has been successfully applied in the optical system of infrared remote sensing. It provides a technical approach for other optical systems to separate the optical spectrum from NIR to LWIR.

Keywords: optical coatings; infrared; dichroic beamsplitter; design and manufacture

1. Introduction

Measurements of radiation at many wavelengths can provide more information about the materials in the selected feature scene, and images can be processed to extract all relevant information contained in multiple spectral bands [1]. As one of the main detection payloads on Earth observation satellites, the infrared multispectral imager has vast applications in meteorological analysis [2], environmental protection [3,4], the exploration of natural resources [5], and early warnings of geological disasters [6,7]. In recent years, because there has been a new generation of photoelectric detection technology that captures image data within specific wavelength ranges throughout the electromagnetic spectrum, multispectral imaging improves the dimension of image information and thus extends the function of traditional detection technology [8]. In a multi-channel infrared remote sensing imaging spectrometer, the spectral response is usually wide, and the instrument needs two or more detectors to detect optical signals of different bands [9]. As one of the important spectral dichroic elements, the dichroic beamsplitter plays a key role in optical path splitting, which is widely used for spectral splitting to change the transmission direction of optical signals in some wave bands so that target signals in different bands can be received by appropriate detectors and then imaged. Figure 1 is a schematic representation of the spectral separation of a dichroic beamsplitter, reflecting SWIR and transmitting MWIR and LWIR. There is a report [10] on the design and construction of a common-aperture multispectral imaging system (CAMIS) to simultaneously obtain spectral data in ultraviolet, visible, MWIR, and LWIR bands. Four dichroic beamsplitters were used to split spectra in different wavelength ranges in the CAMIS. The researchers validated the basic principles of the device by constructing an experimental setup. The spectral splitting function of the dichroic beamsplitters exerted a crucial effect on this system, which had a significant

impact on the integration of the space optical remote sensor. The experimental results indicated that the system could perform celestial navigation in the visible waveband and image objects well in multiple wavebands. The dichroic beamsplitter also has important applications in the military field. Three-channel dichroic beamsplitters, sky cameras, and a main optical system are utilized to identify the wavelengths of the incident laser radiation in the far field [11]. The main contribution of this optical system is to reduce the electronic components and increase the optical components to enhance the signal-to noise ratio by using the dichroic beamsplitter technique with a sky camera detector. In multi-channel infrared imaging systems, an infrared dichroic beamsplitter is fabricated using an optical material commonly represented by a silicon (Si), Ge, or zinc selenide silicon (ZnSe) substrate with multilayer thin films on both sides. To obtain high-quality images, spectral separation must be achieved on one surface, typically the incident surface, and the dichroic beamsplitter must be optically flat. A dichroic coating stack is deposited on one side for the spectral splitting required by the optical system, and the AR coating stack is deposited on the other side for the wavelength range of the transmission area.
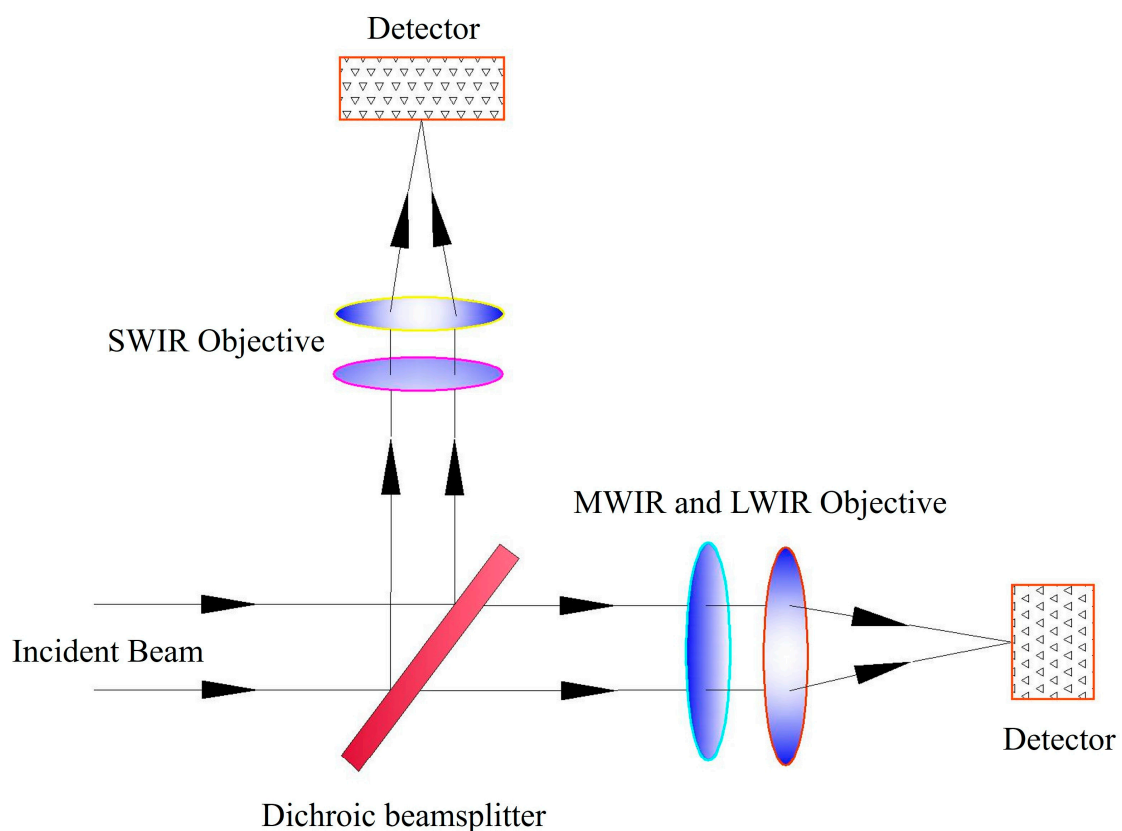
Figure 1. Schematic representation of the spectral separation of the dichroic beamsplitter mounted in optical systems.

So far, some researchers have reported [12–14] on the development of infrared dichroic beamsplitters and obtained excellent research results. A dichroic beamsplitter was designed by Hendrix et al. [15]; band separation occurred on the first optically flat surface, and it separated the SWIR and MWIR bands. A study has been carried out on the design and fabrication of the dichroic coating on zinc selenide flat substrate [16]. The dichroic beamsplitter could separate the 3 to 5 μm and 7.5 to 10.5 μm wavelength regions when it was placed at a 45° angle. Cao et al. [17] developed a dichroic beamsplitter for the laser protection of infrared detectors with a high laser-induced damage threshold. The dichroic beamsplitter protected against 1064 and 532 nm lasers and had high transmittance in the detection beam band of 3.6 to 4.7 μm. Amotchkina et al. [18] developed two beamsplitters operating in the NIR and MWIR spectral ranges; the reflection channel was a band of

0.77 to 1.05 μm and the transmission channels covered wavelengths of 4 to 8 μm. In our previous research report [19], an infrared dichroic mirror based on an infrared dielectric film was able to separate SWIR from LWIR, while the polarization sensitivity was at a relatively low level in the short-infrared range as well as in the long-infrared range. Yu et al. [20] developed a multiplex lens with effective coatings, reflected visible-near infrared (VNIR) and transmitted LWIR, protecting the infrared horizon sensor from solar radiation. However, a dichroic beamsplitter operating at an incidence of 45° to reflect NIR and SWIR and to transmit MWIR and LWIR simultaneously has not been reported to our knowledge, which is the content of our work in this paper. Relying on only one dichroic beamsplitter to achieve spectral separation in the four infrared bands of NIR, SWIR, MWIR, and LWIR has practical significance for optimizing the optical path structure of the system and reducing the weight of the device.

According to the requirements of optical system design, an infrared dichroic beamsplitter divides infrared radiation into SWIR and MW-LWIR by changing the transmission direction. When passing through the dichroic beamsplitter, the NIR channel from 1.28 to 1.38 μm and the SWIR channel from 1.58 to 2.32 μm are reflected in the short-wave detection area, while the MWIR and LWIR channels from 3.7 to 12.5 μm are transmitted into the mid-long-wave detector area. In view of the spectral coverage of a dichroic beamsplitter ranging from NIR to LWIR and the high-reliability demand, the infrared dichroic beamsplitter designed and manufactured for space optical remote sensors poses new challenges for the selection of coating materials and the design of dichroic coatings.

2. Materials and Methods

2.1. Selection of Materials

A dichroic beamsplitter used in the space remote sensing instrument must meet the requirements of spectral separation and have good stability and reliability. Compared to a visible/near-infrared dichroic beamsplitter, the infrared dichroic beamsplitter is manufactured using different materials, and it is difficult to fabricate because of its larger thickness, which also makes it difficult for it to meet the requirements of spatial reliability experiments. In this paper, germanium crystal was selected as the substrate for its wide-spectrum transmission range, excellent optical uniformity, and good mechanical properties. There are only a few kinds of infrared coating materials available that are transparent in the spectrum range from NIR to LWIR. The high-refractive-index materials are Ge and lead telluride (PbTe), which are widely used in infrared optical coatings. Several low-refractive-index materials are optional, including ZnS, ZnSe, and rare-earth fluorides such as YbF_3, yttrium fluoride (YF_3), barium fluoride (BaF_2), thorium fluoride (ThF_4), etc. Among the coating materials mentioned above, PbTe is opaque at wavelengths below 3.2 μm [21], and cannot be used as a high-refractive-index material in the design of dichroic coatings that possess high reflectivity in the short-wave infrared region. ZnS and ZnSe have excellent mechanical and optical properties in the band of 1.2 to 12.5 μm. For another consideration, ZnS has good adhesion to the Ge substrate and good stability between layers according to the results of studies on ZnS thin films. It is a better choice to select commercially available ZnS as a coating material. The surface of the BaF_2 coating is relatively rough, and therefore will generate scattering in the short-wave band. In addition, since the BaF_2 coating is prone to moisture, protective conditions must be considered to meet spatial reliability. At a wavelength greater than 11 μm, the absorption of YF_3 becomes larger [22], significantly affecting the transmittance of the longwave end in the transmission region. Considering that thorium is a radioactive element [23], ThF_4 coating deposition should be carried out under special protective conditions. With excellent optical properties in the band of 1.2 to 12.5 μm and good mechanical properties, YbF_3 without a radioactive element is suitable for dichroic coatings when used as a low-refractive-index material. In this paper, Ge, ZnS, and YbF_3 are selected as coating materials.

In the infrared region, deposited coatings have dispersion and absorption properties. When the infrared transmission spectra of a single-layer coating are fitted with various

dispersion models, optical constants of the coating can be obtained. In this paper, the Lorentz harmonic oscillator model is used as the dispersion model of coating materials. Through this model, fitting the curve of experimental transmission spectrum of all the measured single-layer coatings, optical constants of Ge, ZnS and YbF$_3$ coatings in the infrared band were obtained, as shown in Figure 2. The optical constants of thin-film materials were simulated and fitted in a film design software. This indicates that the substrate temperature had a marked effect on the optical properties of the ZnS and Ge coatings. At a certain temperature, such as 200 °C, the refractive index of the YbF$_3$ coating changes only a little in the SWIR region, while the refractive index of the ZnS and Ge coatings changes greatly. It should be noted that the extinction coefficient of the Ge and YbF$_3$ coating increased when the substrate temperature was below 160 °C.
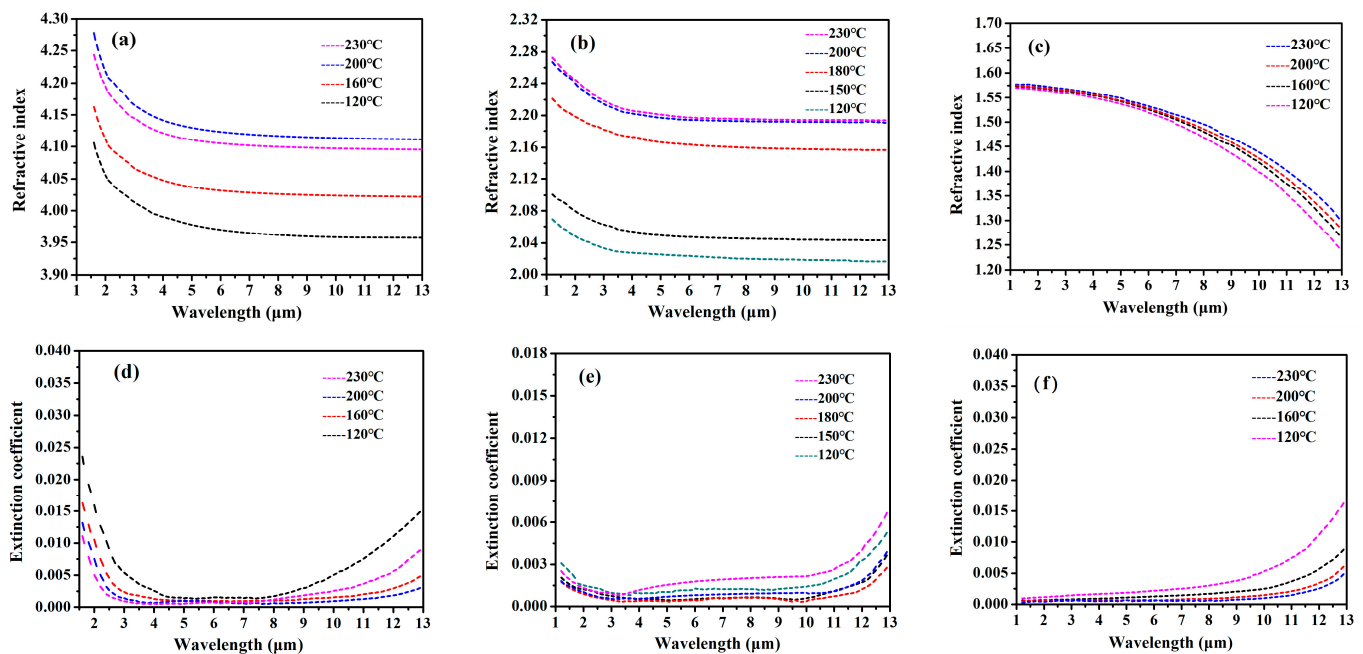
Figure 2. The refractive index of the single-layer Ge coating (**a**), ZnS coating (**b**), and YbF$_3$ coating (**c**), and the extinction coefficient of the single-layer Ge coating (**d**), ZnS coating (**e**), and YbF$_3$ coating (**f**) at different deposition temperatures.

The cross-sectional morphology of the single coating layer of the sample under study was analyzed using a scanning electron microscope (SEM) known as ZEISS SIGMA 500 (Carl Zeiss AG, Oberkochen, Germany). Profile scanning was performed at an accelerating voltage (EHT) of 2.5 kV. The selected magnification was 10,000 times at a work distance of 4.7 mm. Three samples were not coated with a conductive coating such as carbon or Au. In the profile scanning diagram, ZnS, Ge and YbF$_3$ coatings deposited at 200 °C have orderly columnar structures and no obvious defects. The results are presented in Figure 3.
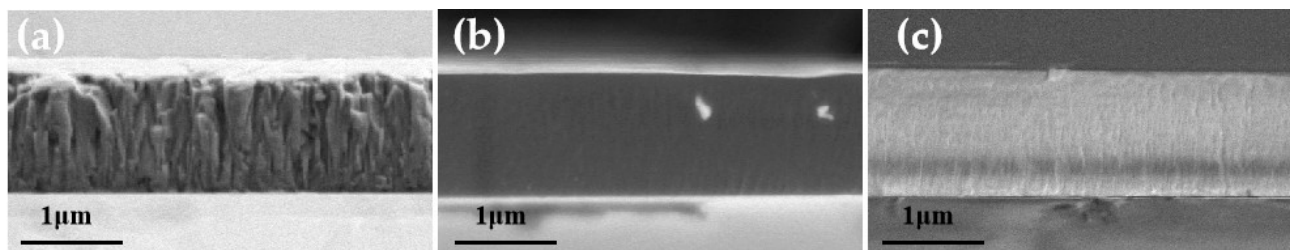
Figure 3. Morphology of the cross-section of sample coatings: the ZnS coating (**a**), Ge coating (**b**), and YbF$_3$ coating, (**c**) deposited at a temperature of 200 °C.

2.2. Optical Coating Design

Three reflection channels distributed within a wide band of 1.28 to 2.32 μm were designated, and multiple transmission channels covering wavelengths from 3.7 to 12.5 μm were required. A reflection stack could not meet the requirements of broad-band reflection, and double reflection stacks were used in the design of dichroic coatings possessing high reflectance. The optimized design of the dichroic coating was made at a 45° angle of incidence. ZnS was used as a low-refractive-index material and Ge was used as a high-refractive-index material in the SWIR reflection band. Taking into account the serious absorption of the Ge coating at a wavelength of 1.58 μm or below, ZnS with low absorption was used as a high-refractive-index material and YbF_3 was used as a low-refractive-index material in the NIR region of the reflection band. The dichroic coatings were composed of a double-reflection stack, that is, Ge/ZnS and ZnS/YbF_3 multilayers. Based on the theory of optical film, the structure of a long-wave pass edge filter was adopted when designed the coating principle. The basic structure of the dichroic coatings is (0.5L H 0.5L)^b, where 0.5 L means a layer of thin film of a low index with an optical thickness of one eighth of the center wavelength, H means a layer of thin film of a high index with an optical thickness of one fourth of the center wavelength, and b is the number of periods. The multilayer reflection stack design was composed of 12-layer Ge/ZnS and 12-layer ZnS/YbF_3 to meet the high reflectivity requirements of the reflection band in NIR and SWIR. To further improve the transmittance of the transmission band and reduce the passband ripple, irregular matching layers were used on both sides of the basic structure and some layers were optimized in multilayers of the dichroic coatings.

In fact, Ge is a high-refractive-index material with about thirty-six percent residual reflectance on one surface of the substrate. When dichroic coatings are deposited on one side of Ge substrate, the other side of the substrate needs to be coated with broad-band antireflection (AR) coatings to obtain high transmittance in the transmission band of 3.7 to 12.5 μm. Another important aspect is that the ghost caused by the surface reflectance of the substrate can be minimized in the optical system via the fabrication of broad-band AR coatings. The antireflective surface of the dichroic beamsplitter was composed of a multi-layer ZnS/Ge/ZnS/Ge/ZnS/YbF_3/ZnS/YbF_3/ZnS broad-band AR coating with low reflectance in the spectral region of 3.7 to 12.5 μm. The details of the thickness of each layer are shown in Table 1. A residual reflectance curve of the designed AR coating is shown in Figure 4a, and it exhibits that the simulated reflectance at a 45° angle of incidence is mainly below 2.7%. After one side of the substrate was coated with AR coatings, the average reflectance of the designed dichroic beamsplitter that had been coated with dichroic coatings on the other side was reduced from 36% to 6.0% in the transmission band, as shown in Figure 4b.

Table 1. The thickness of each layer of the AR coatings.

| Number of Layers	Material	Thickness of Design (nm)
1	ZnS	89.5
2	Ge	201.3
3	ZnS	281.2
4	Ge	106.4
5	ZnS	149.3
6	YbF_3	138.5
7	ZnS	521.6
8	YbF_3	975.9
9	ZnS	50.2

The designed spectral curve is shown in Figure 5a,b, including the theoretical reflectance curve of the reflection channels and the transmittance curve of the transmission channels. The average reflectance of the dichroic beamsplitter in the range from 1.28 to 1.38 μm is 96%, that in the range from 1.58 to 1.83 μm is 98% and that in the range from

1.95 to 2.32 µm is 97.5%, while the average transmittance in the range from 3.7 to 6.2 µm is 94% and that in the range from 7.5 to 12.5 µm is 94.5%. The average reflectance and transmittance of the dichroic beamsplitter can be seen in Table 2.
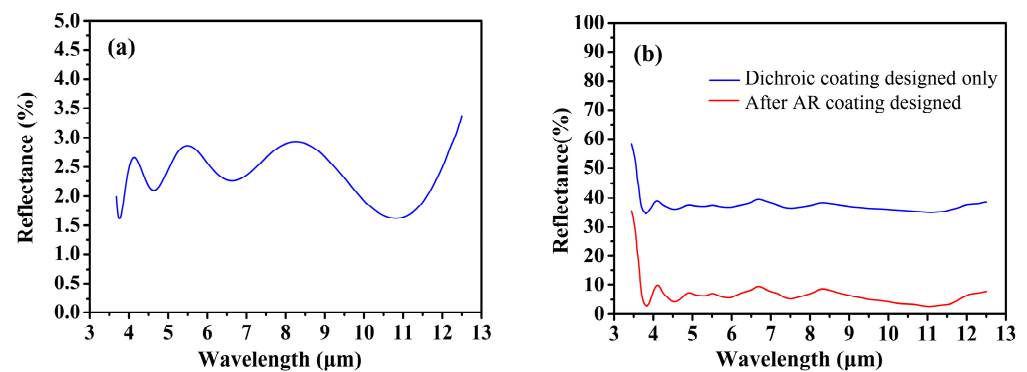
Figure 4. Calculated transmittance of the AR coating (**a**) and dichroic coating (**b**) designed at a 45° angle of incidence on the Ge substrate.
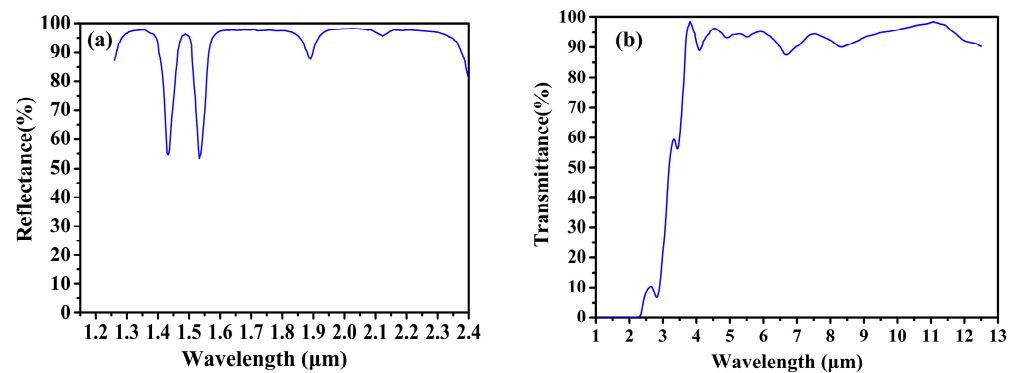
Figure 5. The calculated (**a**) reflectanceand (**b**) transmittance curve of the designed dichroic beamsplitter.

**Table 2.** Design results of the dichroic beamsplitter based on Ge substrate.

Optical Properties	Angle of Inclination	B1	B2	B3	B4	B5
Reflectance	45°	96%	98%	97.5%		
Transmittance	45°				94%	94.5%

B1: average reflectance between 1.28 and 1.38 µm; B2: average reflectance between 1.58 and 1.83 µm; B3: average reflectance between 1.95 and 2.32 µm; B4: average transmittance between 3.7 and 6.2 µm; B5: average transmittance between 7.5 and 12.5 µm.

2.3. Experimentation and Characterization

Both dichroic coatings and AR coatings were deposited in a Leybold ARES 1110 vacuum coating unit. The optical thickness monitoring system works with a Si detector and InGaAs detector, which could detect a wavelength range from 400 to 2500 nm. The ZnS layer was deposited by thermal evaporation with a molybdenum boat. In previous studies, it was discovered that optical properties of ZnS were very sensitive to substrate temperature. It was not conducive to the deposition of ZnS when the substrate temperature was higher than 230 °C. However, when the substrate temperature was lower than 160 °C, the refractive index of ZnS decreased, which was not conducive to the bandwidth control of the shortwave region. Ge and YbF$_3$ layers were deposited via the evaporation of the electron beam. YbF$_3$ layer cracks occurred easily when the temperature was lower than 160 °C, and the absorption in the LWIR region became larger. Experiments showed that the deposition temperature controlled at 200 °C was suitable for the preparation of the dichroic beamsplitter. All coatings were manufactured at a substrate temperature of 200 °C.

The reflectance and transmittance spectra were measured using a flat sample manufactured at the same time as the dichroic beamsplitter was, using Lambda 900 and the Spectrum GX spectrometer from Perkin Elmer, respectively. The measurement angle was 45 deg. The measured optical properties of the sample are shown in Figure 6, including the reflection curve and the transmission spectral curve.
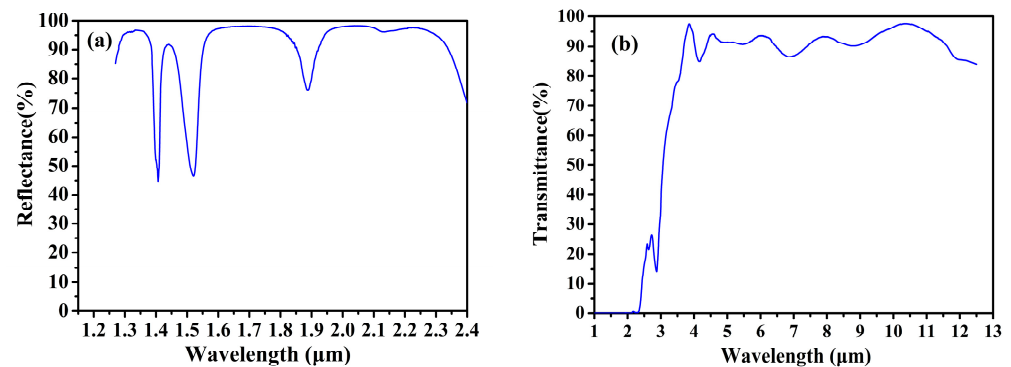
Figure 6. (**a**) Measured NIR and SWIR reflection curves, and (**b**) the wide-infrared transmittance curve of the infrared dichroic beamsplitter.

To verify the reliability of the sample, a water immersion experiment was conducted on the sample. The sample was soaked in pure water and placed in an oven at a constant temperature of 45 °C for 12 h. The sample was taken out, and the surface of the film was observed. The surface of the sample was bright and there was no change in color compared to before it was soaked in water, as shown in Figure 7a,b.
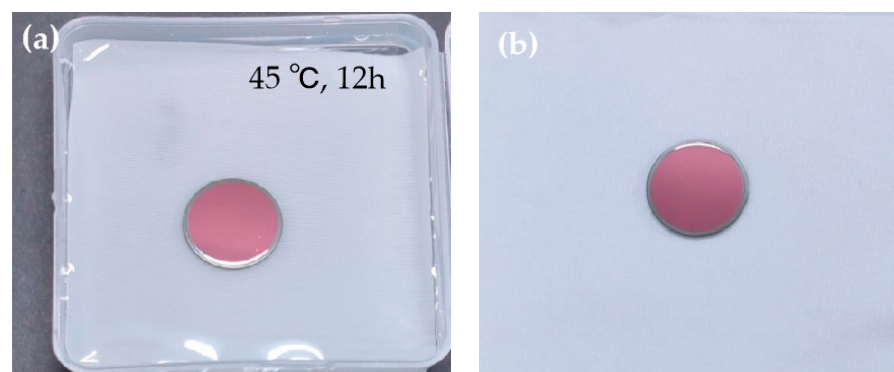
Figure 7. (**a**) Sample soaking experiment, and (**b**) photos of the sample after soaking.

The durability of the sample was determined under further experimental conditions, including rapid tearing with adhesive tape (adhesive tape size: 1 × 1 cm), a temperature test (maintained at a temperature of −50 °C and 60 °C for 2 h 3 times) and a damp heat test (maintained at 47 °C and 95% relative humidity for 24 h continuously). These conditions indicated that the sample could endure all the tests.

3. Results and Discussion

Given that the optical transmission efficiency and reliability of the dichroic beamsplitter are key technical indicators for its engineering applications, closely related goals and results are the focus of our study. The more periods a reflective stack is used in design, the higher the reflectivity of the reflective band. However, a higher number of periods will result in larger ripple in the passband of the transmission band. In addition, the increase in film thickness is also not conducive to the reliability control of the dichroic coatings, so the number of reflector periods in the design of the dichroic coating is strictly limited. The design of the dichroic beamsplitter utilized reflective stacks with different material combinations, and involved the selection of six-period reflective stacks in the reflective

band to achieve high reflectivity while minimizing the total thickness of the film. The optimization of some dichroic coating and matching layers, and the design of the AR coating on the surface of the opposite side are important for improving the transmittance of the dichroic beamsplitter in MWIR and LWIR and in compressing the transmission band ripple. The measured average reflectance of the dichroic beamsplitter in the range from 1.28 to 1.38 μm is 95%, that in the range from 1.58 to 1.83 μm is 97% and that in the range from 1.95 to 2.32 μm is 96.5%, while the average transmittance in the range from 3.7 to 6.2 μm is 92% and that in the range from 7.5 to 12.5 μm is 92%. The average reflectance and transmittance of the dichroic beamsplitter can be seen in Table 3. The measurement of reflection and transmission spectra shows that the dichroic beamsplitter achieved satisfactory optical transfer efficiency in both the reflection and transmission bands. There is an evident discrepancy, especially between the designed and measured reflection. It should be noted that the transmittance of the band decreased at wavelengths greater than 11.5 μm. One reason is that there was lattice vibration absorption in the Ge substrate at wavelengths greater than 11.5 μm. The other cause is that the cumulative monitoring error in coating depositing affected the waveform of the transmission band. After all environmental tests were completed, both the dichroic and AR coatings did not blister, crack, or fall off. The optical properties of the sample remained almost unchanged after environmental tests. This was a satisfactory result for the space remote sensor.

Table 3. Measured results of dichroic beamsplitter based on Ge substrate.

Optical Properties	Angle of Inclination	C1	C2	C3	C4	C5
Reflectance	45°	95%	97%	96.5%		
Transmittance	45°				92%	92%

C1: average reflectance between 1.28 and 1.38 μm; C2: average reflectance between 1.58 and 1.83 μm; C3: average reflectance between 1.95 and 2.32 μm; C4: average transmittance between between 3.7 and 6.2 μm; C5: average transmittance between between 7.5 and 12.5 μm.

A reliability environment simulation test was conducted on the designed and manufactured dichroic beam splitter to ensure that the thin-film components met the reliability requirements of in-orbit operation. The dichroic beamsplitter passed all the following reliability tests, as shown in Table 4.

Table 4. A reliability environment simulation test on the dichroic beamsplitter.

Test Content	Temp. Humidity Test	Soaking Test	Adhesion Test	Temp. Alternating Test
Test conditions	47 °C air humidity is 95%, maintained for 24 h	45 °C for 12 h in a baking oven	rapid tearing adhesive tape size: 1 × 1 cm	−50 °C and 60 °C for 2 h; 3 times liquid nitrogen
Results	passed	passed	passed	passed

Our research contributes to the optimization of the optical path structure and to reducing the weight of the payload in the space optical remote sensor by using only one dichroic beamsplitter to achieve spectral separation in the four infrared bands, NIR, SWIR, MWIR, and LWIR, that need to be covered by the optical path system. The dichroic beamsplitter designed and manufactured in our work efficiently reflects NIR and SWIR, while also exhibiting a high transmission of MWIR and LWIR. The dichroic beamsplitter designed and manufactured in our research was successfully used in a space optical remote sensor.

4. Conclusions

A dichroic beamsplitter based on Ge substrate, possessing optical properties of reflection of the wave range from NIR to SWIR and transmitting MWIR and LWIR, was

designed and manufactured for the space optical remote sensor. The dichroic beamsplitter passed the 45 °C water immersion experiment. It could also withstand the requirements of environmental tests, including high-humidity and high- and low-temperature alternation, and is capable of meeting the demanding space requirements. It provides a technical approach for the development of infrared dichroic beamsplitters in other engineering projects. With the increasing performance requirements of some space remote sensing sensors, the working wavelength of the dichroic beamsplitter is hoped to be expanded, and higher optical transfer efficiency for reflection and transmission is required when the system has high requirements for imaging quality. It can be seen that the development of dichroic beamsplitters has become more challenging, which means that researchers need to invest more energy in the design and manufacturing of dichroic beamsplitters.

Author Contributions: Conceptualization, L.J. and T.Y.; methodology, L.J. and Y.Q.; investigation, T.Y., W.D. and D.L.; performance testing, L.J. and Y.Q.; data analysis, T.Y.; writing—original draft preparation, L.J.; writing—review and editing, T.Y. and W.D. All authors have read and agreed to the published version of the manuscript.

Institutional Review Board Statement: Not applicable.

Informed Consent Statement: Not applicable.

Data Availability Statement: No new data were created or analyzed in this study. Data sharing is not applicable to this article.

Conflicts of Interest: The authors declare that there are no conflicts of interest regarding the publication of this manuscript.

References

1. Huang, L.Q.; Luo, R.C.; Liu, X.; Hao, X. Spectral imaging with deep learning. *Light. Sci. Appl.* **2022**, *11*, 61. [CrossRef] [PubMed]
2. Kim, Y.; Ryu, H.S.; Hong, S. Data-to-data translation-based nowcasting of specific sea fog using geostationary weather satellite observation. *Atmos. Res.* **2023**, *290*, 106792. [CrossRef]
3. Hawkins, G.; Sherwood, R.; Djotni, K.; Coppo, P.; Höhnemann, H.; Belli, F. Cooled infrared filters and dichroics for the sea and land surface temperature radiometer. *Appl. Opt.* **2013**, *52*, 2125–2135. [CrossRef]
4. Kouli, M. Editorial for the special issue "Application of Satellite Remote Sensing in Solving Urban Geo-Environmental Issues". *Remote Sens.* **2023**, *15*, 63. [CrossRef]
5. Chen, H.; Xie, X.B.; Liu, E.Q.; Zhou, L.; Yan, L.J. Application of infrared remote sensing and magnetotelluric technology in geothermal resource exploration: A case study of the wuerhe area, Xinjiang. *Remote Sens.* **2021**, *13*, 4989. [CrossRef]
6. Taquet, N.; Meza Hernández, I.; Stremme, W.; Bezanilla, A.; Grutter, M.; Campion, R.; Palm, M.; Boulesteix, T. Continuous measurements of SiF_4 and SO_2 by thermal emission spectroscopy: Insight from a 6-month survey at the Popocatépetl volcano. *J. Volcanol. Geotherm. Res.* **2017**, *341*, 255–268. [CrossRef]
7. Shu, A.Q.; Shen, F.F.; Jiang, L.P.; Zhang, T.; Xu, D.M. Assimilation of Clear-sky FY-4A AGRI radiances within the WRFDA system for the prediction of a landfalling Typhoon Hagupit. *Atmos. Res.* **2023**, *283*, 106556. [CrossRef]
8. Zhou, S.; Zhang, L.Y.; Guo, F.; Wu, C.F.; Xu, J.Q.; Zhang, K.F.; Li, K.; Liu, Z.; Xiao, X.G.; Song, S.G.; et al. Design and fabrication of an integrated dual-channel thin-film filter for the mid-infrared. *Coatings* **2021**, *11*, 803. [CrossRef]
9. Duan, W.B.; Liu, B.J.; Zhuang, Q.H.; Jiang, L.; Li, D.Q.; Yu, D.M.; Qin, Y.; Ni, R.; Li, Y.P.; Zhou, S.; et al. Research Progress of infrared thin film coatings applied in space remote sensing systems. *Acta Photon. Sin.* **2022**, *51*, 0951601.
10. Cao, J.J.; Chang, J.; Huang, S.; Wu, Y.N.; Ji, Z.Y.; Lai, X.X.; Wang, J.Y.; Li, Y.T.; Zhu, W.H.; Li, X.Y. Optical design and fabrication of a common-aperture multispectral imaging system for integrated deep space navigation and detection. *Opt. Laser Eng.* **2023**, *167*, 107169. [CrossRef]
11. Mohamed, A.A.A.; Ahmed, M.; Shehata, M.; Almslmany, A. A novel dichroic beam splitters and sky cameras-based LIDAR receiver. In Proceedings of the IEEE International Telecommunications Conference (ITC-Egypt), Alexandria, Egypt, 13–15 July 2021; pp. 1–4.
12. Mahendra, R.; Chandra, R. Dichroic beam splitter for visible, short-wave infrared, and mid-wave infrared. *Opt. Eng.* **2022**, *61*, 105111. [CrossRef]
13. Rothhardt, C.; Birckigt, P.; Grabowski, K.; Risse, S.; Schlegel, R.; Shestaeva, S.; Schwinde, S.; Schmidl, S.; Klose, S. Realizing an all-glass beam splitter for space by using advanced joining technologies. *Proc. SPIE* **2022**, *12777*, 1277719.

14. Li, H.R.; Yang, R.S.; Xie, L.Y.; Wei, Z.Y.; Zhang, J.L.; Wang, Z.S.; Cheng, X.B. Scattering characteristics of various nodular defects in a dichroic beam splitter. *Opt. Express* **2024**, *32*, 949–958. [CrossRef] [PubMed]

15. Hendrix, K.; Kruschwitz, J.D.; Keck, J. Optical interference coatings design contest 2013: Angle-independent color mirror and shortwave infrared/mid-wave infrared dichroic beam splitters. *Appl. Opt.* **2014**, *53*, 360–374. [CrossRef] [PubMed]

16. Upadhyaya, A.S.; Ghosh, A.; Bandyopadhyay, P.K. Short wave pass and long wave pass dichroic coating at 45° on zinc selenide substrate for dual band thermal imager. *Infrared Phys. Technol.* **2009**, *52*, 146–151. [CrossRef]

17. Cao, J.; Jiang, B.B.; Jiao, H.F.; Niu, X.S.; Zhang, J.L.; Zhang, Z.; Chen, X.B.; Wang, Z.S. A dichroic beamsplitter for the laser protection of infrared detectors. *Coatings* **2022**, *12*, 1861. [CrossRef]

18. Amotchkina, T.; Trubetskov, M.; Schulz, M.; Pervak, V. Comparative study of NIR-MIR beamsplitters based on ZnS/YbF$_3$ and Ge/YbF$_3$. *Opt. Express* **2019**, *27*, 5557–5569. [CrossRef] [PubMed]

19. Jiang, L.; Qin, Y.; Cai, Q.Y.; Liu, D.Q.; Yu, T.Y. Study for low-polarization-sensitive dichroic mirrors to space remote sensing. *Proc. SPIE* **2022**, *12169*, 1216990.

20. Yu, T.Y.; Liu, D.Q.; Qin, Y. The coatings for a solar-rejected window of the infrared horizon sensor. *Infrared Phys. Technol.* **2020**, *105*, 103214. [CrossRef]

21. Stolberg-Rohr, T.; Hawkins, G.J. Spectral design of temperature-invariant narrow bandpass filters for the mid-infrared. *Opt. Express* **2015**, *23*, 580–596. [CrossRef]

22. Liu, H.S.; Li, S.D.; Chen, D.; Yang, X.; He, J.H.; Jiang, Y.G.; Wang, L.S.; Liu, D.D.; Ji, Y.Q. Study on broadband optical constants of yttrium fluoride thin films deposited by electron beam evaporation. *Optik* **2020**, *205*, 163548. [CrossRef]

23. Kumar, R.; Sonal, G.; Wajhal, S.; Satpati, S.K.; Sahu, M.L. Effect of process parameters on the recovery of thorium tetrafluoride prepared by hydrofluorination of thorium oxide, and their optimization. *Nucl. Eng. Technol.* **2022**, *54*, 1560–1569. [CrossRef]